Evaluation of InGaN/GaN light-emitting diodes of circular geometry

X.H. Wang, W.Y. Fu, P.T. Lai and H.W. Choi*

Semiconductor Display and Lighting Laboratory, Department of Electrical and Electronic Engineering
The University of Hong Kong, Pokfulam Road, Hong Kong
** hwchoi@hku.hk*

Abstract: Blue GaN light emitting diodes (LEDs) in the shape of cuboids and circular disks have been fabricated by laser micromachining. The proposed circular geometry serves to enhance overall light extraction on a macro-scale and to improve uniformity of the emission pattern due to the rotational symmetry of the chip. Analysis of the chip shaping effect is carried out by ray-tracing simulations and further supported with mathematical modeling using ideal LED models, and subsequently verified with fabricated devices. In comparison, a 10% improvement in overall emission was observed for circular LEDs over the regular cuboids, consistent with simulations and calculations. The measured emission pattern from the circular LED confirms the axial symmetry of the emission beam.

OCIS codes: (220.0220) Optical design and fabrication; (230.3670) Light-emitting diodes.

References and links

1. D. S. Han, J. Y. Kim, S. I. Na, S. H. Kim, K. D. Lee, B. Kim, and S. J. Park, "Improvement of light extraction efficiency of flip-chip light-emitting diode by texturing the bottom side-surface of sapphire substrate," IEEE Photon. Technol. Lett. **18**(13), 1406–1408 (2006).
2. T. Fujii, Y. Gao, R. Sharma, E. L. Hu, S. P. DenBaars, and S. Nakamura, "Increase in the extraction efficiency of GaN-based light-emitting diodes via surface roughening," Appl. Phys. Lett. **84**(6), 855–857 (2004).
3. H. W. Choi, M. D. Dawson, P. R. Edwards, and R. W. Martin, "High extraction efficiency InGaN micro-ring light-emitting diodes," Appl. Phys. Lett. **83**(22), 4483–4485 (2003).
4. S. X. Jin, J. Li, J. Y. Lin, and H. X. Jiang, "InGaN/GaN quantum well interconnected microdisk light emitting diodes," Appl. Phys. Lett. **77**(20), 3236–3238 (2000).
5. W. N. Ng, C. H. Leung, P. T. Lai, and H. W. Choi, "Photonic crystal light-emitting diodes fabricated by microsphere lithography," Nanotechnology **19**(25), 255302 (2008).
6. P. Royo, R. P. Stanley, and A. Ilegems, "Analytical Calculation of the Extraction Efficiency of Microcavity Light-Emitting Diodes for Display and Fiber Coupling Applications," IEEE J. Sel. Top. Quantum Electron. **8**(2), 207–218 (2002).
7. D. S. Liu, T. W. Lin, B. W. Huang, F. S. Juang, P. H. Lei, and C. Z. Hu, "Light-extraction enhancement in GaN-based light-emitting diodes using grade-refractive-index amorphous titanium oxide films with porous structures," Appl. Phys. Lett. **94**(14), 143502 (2009).
8. C. Wiesmann, K. Bergenek, N. Linder, and U. T. Schwarz, "Photonic crystal LEDs – designing light extraction," Laser Photonics Rev. **3**(3), 262–286 (2009).
9. W. Y. Fu, K. N. Hui, X. H. Wang, K. K. Y. Wong, P. T. Lai, and H. W. Choi, "Geometrical Shaping of InGaN Light-emitting Diodes by Laser Micromachining," IEEE Photon. Technol. Lett. **21**(15), 1078–1080 (2009).
10. C. C. Kao, H. C. Kuo, H. W. Huang, J. T. Chu, Y. C. Peng, Y. L. Hsieh, C. Y. Luo, S. C. Wang, C. C. Yu, and C. F. Lin, "Light-output enhancement in a nitride-based light-emitting diode with 22 degrees undercut sidewalls," IEEE Photon. Technol. Lett. **17**(1), 19–21 (2005).
11. X. H. Wang, P. T. Lai, and H. W. Choi, "Laser Micro-machining of Optical Microstructures with Inclined Sidewall Profile," J. Vac. Sci. Technol. B **27**(3), 1048–1052 (2009).

1. Introduction

The external light extraction efficiency had been the bottle neck of the overall efficiency of visible and ultraviolet (UV) GaN light-emitting diodes (LEDs) due to the relatively high refractive index of the semiconductor material. A great amount of the light emission from the quantum wells is lost within the GaN layer due to light confinement and subsequent re-absorption. Many methods have been proposed to improve the light extraction rate, such as surface roughing [1,2], micro-patterning [3,4], nanopatterning [5], microcavity LED design

#116072 - $15.00 USD Received 24 Aug 2009; revised 6 Nov 2009; accepted 16 Nov 2009; published 23 Nov 2009

[6], coating of porous films [7] and photonics crystals [8] etc. Recently, the effect of geometrical chip-shaping realized with laser micromachining or other methods is gradually being recognized as a promising alternative technique for optimizing efficiency and for modulation of the emission pattern [9,10].

Lasers are flexible and versatile tools used in the micromachining and precision manufacturing of miniature components as small as several micrometers. Laser micromachining has been applied in medical and biotechnology research to process a wide range of materials ranging from polymers, metals, ceramics, glass and semiconductors. Micromachining of hard photonic materials, such as sapphire, is an indispensible procedure in LED fabrication and packaging, excelling in the capability of shaping precision freedom structures, such as a circular LED proposed in this work, which would otherwise have been impossible with conventional wafer sawing techniques. In this paper, we demonstrate a circularly-shaped LED chip machined with laser beams; pronounced improvement to the sidewall light extraction ratio as well as angular uniformity of the emission pattern was achieved, based on simulations, calculations and measurements.

2. Experimental details

Our experimental set-up for laser micromachining comprises of a nanosecond diode-pumped solid-state UV laser source at 349 nm, focused with a triplet lens onto a sample placed on an x-y-θ motorized translation platform. Details of this set-up have previously been reported [11]. The LEDs were fabricated using standard micro-fabrication procedures. The emissive regions of individual LED chips are 500 μm x 500 μm. Chips of cuboid geometry were diced by regular laser micromachining, with the beam translating along the axis of the device. The circular LED structure was formed by rotary micromachining, whereby the LED chip was precisely located at the centre of rotation. The laser micromachining was performed with the GaN-side facing upwards and the efficiency was optimized by focusing the beam to a tight spot onto the sample top surface. The laser processing efficiency also depends on the laser pulse energy, pulse width, beam characteristics, the optical quality of the focusing optics and the thickness of the sapphire substrate amongst other factors. With the laser operated at a pulse repetition rate of 1 kHz and 90 μJ pulse energy, a single or double scan passes at a translation speed of 50 μm/sec is sufficient to penetrate a 200 μm thick sapphire wafer for complete separation. For ray-tracing simulation using Tracepro, the layout of the LED models is simplified with both metal pads removed to shorten the simulation times. All surfaces of the LED under simulation are modeled to be of optical quality. Light radiation from the multi-quantum wells (MQWs) with uniform angular distribution travels through the materials and across interfaces according to Snell's law. The optical properties at 475 nm adopted in the simulation are listed in Table 1.

Table 1. Optical parameters adopted in simulations (at 475 nm).

Layer	Thickness (nm)	Refractive Index	Absorption (mm^{-1})
Sapphire	3.2×10^5	1.78	0
GaN	4000	2.42	15
MQW	200	2.44	15

#116072 - $15.00 USD Received 24 Aug 2009; revised 6 Nov 2009; accepted 16 Nov 2009; published 23 Nov 2009

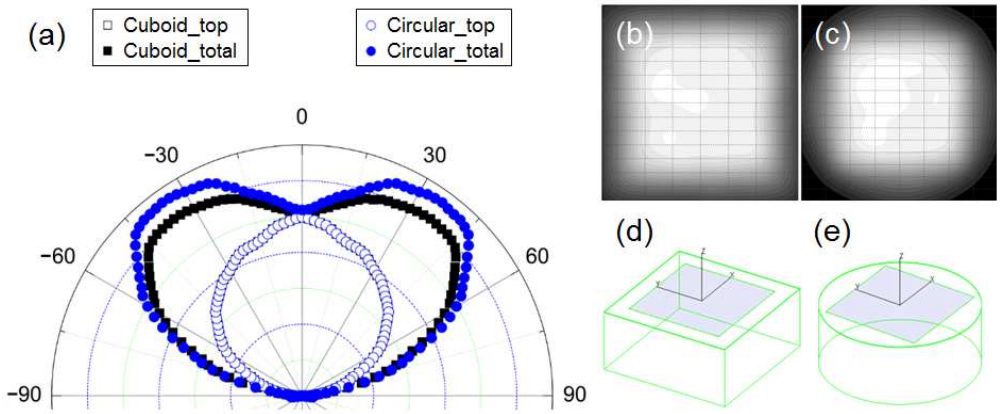

Fig. 1. (a) The simulated emission patterns obtained from ray tracing using LED models of cuboid and circular disk geometries, both have an emissive region of 500 µm x 500 µm. The light extraction efficiency was determined to be 12.47% and 13.43% respectively, corresponding to an overall enhancement of ~7.8% due to enhanced sidewall extraction efficiency. The extraction ratios from top-surfaces are ~83% for both models, while the circular sidewall is capable of delivering a higher extraction ratio of 52%, ~19% higher than the cuboid geometry. The simulated spatial intensity patterns at a plane near the top surfaces of the LEDs are plotted in parts (b) and (c). The corresponding models used in the simulations are illustrated in parts (d) and (e).

In order to carry out a fair comparison, the modeled LEDs of cuboid and circular geometries have identical light emission areas, and that their volumes are equal. The simulated emission patterns are plotted in Fig. 1(a), whereby the overall light extraction efficiencies are 12.47% and 13.43% respectively for cuboid and circular LED geometries. The relative light output is thus predicted to be enhanced by nearly 7.8%. To obtain angular emission patterns of the packaged devices experimentally, a photodetector was rotated about an axis in the XY plane above the device, in steps of 2°, while the output powers were measured through an integrating sphere.

3. Results and discussions

According to Snell's law, rays propagating within an escape cone defined by the difference in refractive index at an interface can cross the boundary (minus reflection) while rays beyond the cone are totally reflected. In the case of a cavity with vertical side walls, the angle a light ray makes with the normal does not change even after multiple reflections from the planer interfaces or the vertical side walls. Light emits from the MQW regions of an LED in a pattern of uniform radiant intensity in all directions. Light emission angle can be divided into 4 regions separated by 3 pairs of cones as drawn in Fig. 2(a). The half angle γ_1 of ~24.4° is determined by the refractive index difference between GaN and air. With a uniform radiation pattern, light rays in cone γ_1 account for 8.9% of the total light output from MQWs. Radiation within cone γ_1 will escape from the top surface, as illustrated in Fig. 2(b), with an extraction ratio of 83%. Rays beyond the half angle γ_2 of 37.5° would be refracted at the GaN/Sapphire interface and have a chance to reach the sidewall at an incident angle smaller than the critical angle defined by the refractive index difference between sapphire and air. Examples of such rays are depicted in Fig. 2(c). Finally, γ_3 = 47.4° defines the escape cone within which light can be transmitted from GaN to the sapphire substrate. Therefore, light rays between angles γ_2 and γ_3 account for 11.6% of total emission and contribute to sidewall light extraction. Table 2 lists the simulated light extraction rates from the top and sidewall surfaces of a cuboid LED and a circular disc LED with emission areas of 500 x 500 µm^2, assuming ideal glossy surfaces. In both cases the ratio between chip area and light-emission area is maintained at ~0.75, while the thicknesses of both chips are 320 µm. The overall light extraction from an

#116072 - $15.00 USD Received 24 Aug 2009; revised 6 Nov 2009; accepted 16 Nov 2009; published 23 Nov 2009

LED is composed of direct top-surface emissions and also emissions from the sidewall regions. From the calculated figures listed in Table 2, the overall enhancement factor of the circular LED is 7.8% over the rectangular counterpart, which is mainly attributed to enhanced sidewall extraction from the curved surface. Considering just sidewall emissions alone, an enhancement factor of 19.1% was obtained, while the top-surface light extraction rates are identical for both the cuboid and circular chips. According to the simulation results, the sidewall extraction ratios within the region from γ_2 to γ_3 are 43.3% and 51.5% for cuboid and circular geometry respectively. It can be seen that the light extraction efficiency from sidewalls is indeed dependent on the device geometry, and a circular shape is just one of many potential designs capable of improving device performance. Circular LED dies can be hexagonally closed-packed on a wafer to minimize loss of chip space.

An additional simulation was performed for circular and rectangular LEDs with emission areas of 300 x 300 μm^2 to investigate the effects of dimensional scaling, the results of which are also shown in Table 2. The dimensions of the chips were scaled down proportionally to maintain the ratio 0.75 between chip area and light-emission area, while the thicknesses were kept at 320 μm. It was found that the overall light extraction rates increases slightly for smaller devices for LEDs of both geometries. This is mainly attributed to increased sidewall extraction as a result of reduced absorption due to shorter optical paths.

Table 2. Simulated light extraction rates from LEDs of different geometries and dimensions.

Shape of LED chip	Rectangular	Circular	Rectangular	Circular
Mesa dimension/ μm^2	500 × 500	500 × 500	300 × 300	300 × 300
Top surface extraction	7.44%	7.45%	7.50%	7.52%
Sidewall extraction	5.02%	5.98%	5.64%	6.70%
Overall extraction	12.47%	13.43%	13.14%	14.22%

It is worthwhile focusing on light extraction selectively from the sidewall, corresponding to γ angles of 30°~50° in the emission plot as shown in Fig. 3(a). It is noted that rays escaping from the sidewall are mostly directed into the lower hemisphere of the distribution plot, which are subsequently reflected by the mirror-coated package into the upwards direction. The most efficient sidewall extraction route is denoted by the green ray in Fig. 2(c), whereby the allowed ray reaches the sapphire sidewall without reflection and with minimum power loss. This is verified by the ray-tracing plot in Fig. 3(b) whereby the intensities of light rays are represented by colors, red being the highest. Sidewall extracted rays of the highest intensities are mostly directed downwards, and subsequently reflected by the bottom mirror reflector.

#116072 - $15.00 USD Received 24 Aug 2009; revised 6 Nov 2009; accepted 16 Nov 2009; published 23 Nov 2009

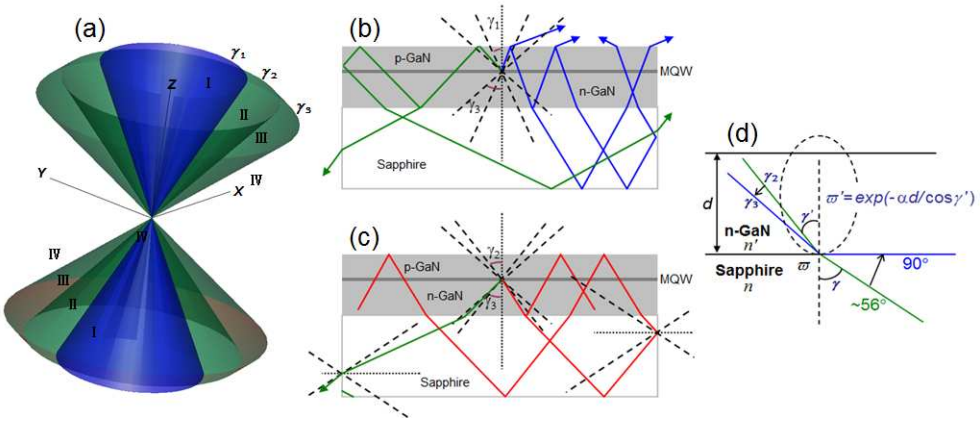

Fig. 2. Light emissions from the MQW layers can be divided into 4 regions separated by 3 cones as shown in (a). Light rays within the first escape cone γ_1 are extracted through the top surfaces exhibited by blue rays in (b). Light rays in the region between cone γ_2 and γ_3 contribute to sidewall extraction as traced with green rays both in (b) and (c). Rays beyond cone γ_3 is confined within GaN and those between cone γ_1 and γ_2, shown as red rays, are forbidden to escape due to total internal reflection on the sidewall. (d) Schematic diagram showing the oval angular intensity distribution of the optical power that reaches the interface of n-GaN/Sapphire after considering the effects of absorption.

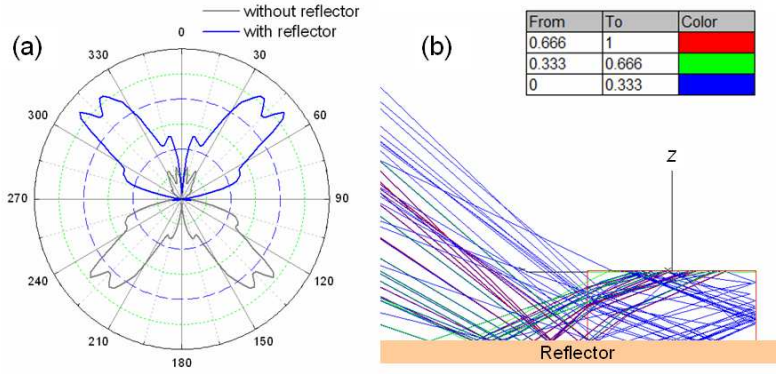

Fig. 3. (a) Sidewall emission pattern of a circular LED model with and without a bottom mirror reflector. (b) Selected rays from simulation illustrating the directionality of sidewall extractions. Colors of rays indicate optical power (decreasing power from red to blue).

The simulation result is then verified with fabricated devices. Figure 4(a) and 4(b) shows microphotographs of the two emitters biased at 1 mA. Figure 5 plots the optical output power as a function of current injection. Each set of result is averaged over 3 measured devices fabricated from the same wafer for a fair and accurate comparison. The circular LED emits 10.3% more light on average in comparison to the cuboid LED, which is slightly higher than the simulation results (of 7.8%). This discrepancy may be partially induced by scattering across dispersive sapphire sidewall, roughened by the laser process. According to simulation results, most sidewall extracted rays are directed downwards. However, the emission image in Fig. 4 indicates a significant proportion of upward-emitting rays from the sapphire sidewall. In fact, all rays within cone γ_3 are more or less scattered by the sidewall, improving chances of escaping directly through the side wall or from the top surface. In any case, although a rough surface modifies the emission characteristics, it generally promotes light extraction and homogenizes the angular distribution of light extractions.

#116072 - $15.00 USD Received 24 Aug 2009; revised 6 Nov 2009; accepted 16 Nov 2009; published 23 Nov 2009

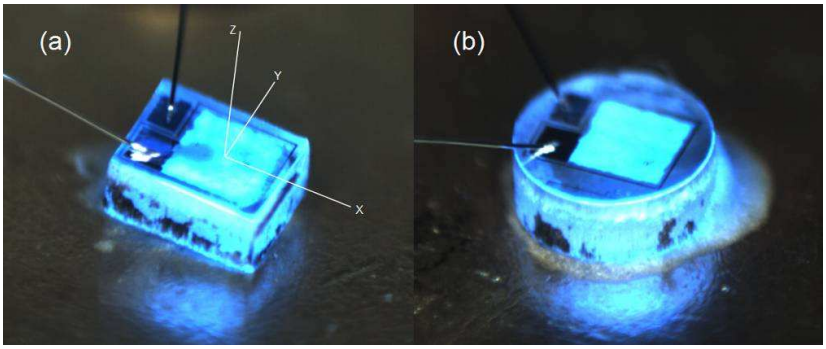

Fig. 4. Optical microphotographs of (a) cuboid and (b) circular LEDs fabricated with laser micromachining. The devices are biased at 1 mA current.

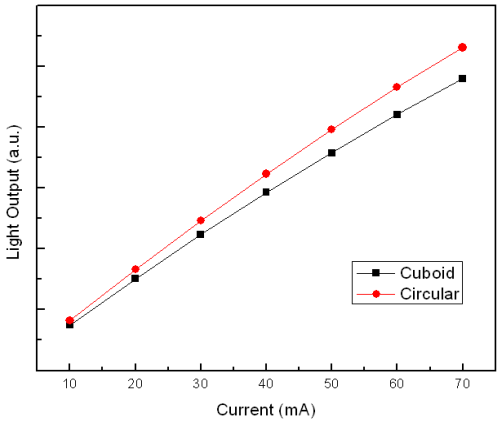

Fig. 5. L-I characteristics of the laser micro-machined cuboid LED and circular LED. Circular LED outputs 10.3% more optical power on average than the cuboid LED at the same current level.

The mechanism of geometric effect on sidewall light extraction is further analyzed with the aid of the schematic diagrams in Fig. 6. As the reflectivity is relatively small and usually lead to additional absorption within the semiconductor layer, multiple-reflected rays are neglected in the following discussion. In Fig. 6(a), point **S** is a point light source located at the interface of GaN and sapphire, and $\mathbf{SP}_1$ and $\mathbf{SQ}_2$ are two representative light rays propagating towards the planar sidewall of a cuboid LED incident at points $\mathbf{P}_1$ and $\mathbf{Q}_2$ respectively. The angle these rays make with the vertical line $\mathbf{SS}_1$ is γ. **P** and **Q** are the projected points of $\mathbf{P}_1$ and $\mathbf{Q}_2$ on the plane of the GaN-sapphire interface and **SP** is perpendicular to the plane of the sidewall; correspondingly, the incident angle of beam $\mathbf{SP}_1$ is at minimum (of 90°-γ). As the projected angle φ between **SP** and **SQ** increases, the incident angle of beam $\mathbf{SQ}_2$ on the sidewall approaches the critical angle γ_c (of ~34°) for total internal reflection (TIR) at sapphire/air interface and the corresponding angle φ_c as marked in the horizontal 2-dimensional diagram of Fig. 6(b) is solved as Eq. (1):

$$\phi_c = \arccos\left(\frac{\cos\gamma_c}{\sin\gamma}\right) = \arccos\left(\frac{\sqrt{1-1/n^2}}{\sin\gamma}\right) = \arccos\left(\frac{\sqrt{n^2-1}}{n'\sin\gamma'}\right) \qquad (1)$$

where $\boldsymbol{n}$ and $\boldsymbol{n'}$ are the refractive indexes of sapphire and GaN respectively. It can be seen that φ_c is determined by γ, which is related to γ' in GaN through Snell's law. For a specific angle γ, the proportion of light rays that can be extracted through the four sidewall facets of a cuboid

#116072 - $15.00 USD Received 24 Aug 2009; revised 6 Nov 2009; accepted 16 Nov 2009; published 23 Nov 2009

structure are within the angles in the white-shaded regions and account for $8\varphi_c/2\pi$ of the total beam cone.

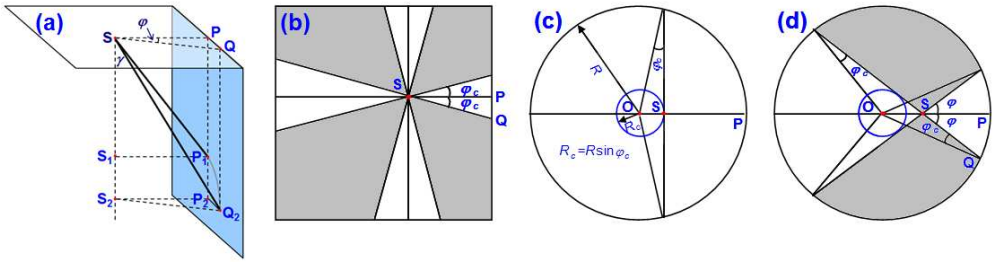

Fig. 6. (a) 3-dimentional schematic diagram illustrating two possible light rays SP_1 and SQ_2 that can be extracted through the planar sidewall, propagating from point S along the emission cone. (b) The projected image of the light rays in (a) onto a horizontal plane. Rays falling within the unshaded region can be extracted; (c) All light rays can be extracted when point source S is within the central circular region defined by R_c for a circularly-shaped sidewall. (d) When point source S is located beyond the central region R_c, only rays within the unshaded regions can be extracted.

In the case of a circular LED with radius R, the portion of light that can be extracted depends on the distance from the emission point source to the centre of the circle. If the source **S** is located within the the small circle region defined by R_c in diagram (c) of Fig. 6, all light rays can be extracted in any direction. When the light source falls out with the aforementioned circle, only part of the light rays can escape as illustrated in Fig. 6(d). The entire span of angles for which light can be extracted account for $4\varphi/2\pi$ of the beam cone, where φ is determined with the following Eq. (2):

$$\phi = \arcsin\left(\frac{R\sin\phi_c}{r}\right) = \arcsin\left(\frac{R_c}{r}\right) \tag{2}$$

Our analysis is based on a circular light emission area which lies concentric with the circular LED chip with radius R and that the radius of the active region r is larger than R/n, the maximum R_c of the circular LED. All rays which can be extracted radiate from the circular light emitting area with radius r are weighted by the extraction ratio and are integrated to estimate the overall sidewall extraction efficiency in a circular LED; the same was carried out for a cuboid LED for comparison. The range of angles (between γ_2 and γ_3) in the GaN layer that contributes to sidewall extraction is depicted in Fig. 2(d). By considering the absorption of GaN, the angular intensity distribution evolves from a uniform circular pattern to that of an oval pattern at the GaN/sapphire interface according to the following relation:

$$\varpi' = \exp(-\alpha d / \cos\gamma')$$

where α and d are the absorption coefficient and thickness of the GaN layer. The magnitude of sidewall extraction of cuboid LED and circular LED are estimated by the definite integrals in Eqs. (3) and (4) respectively:

$$\begin{aligned}\Phi_{sidewall}^{cuboid} &= \int_{\gamma_2}^{\gamma_3} \varpi' \cdot T \int_0^r \left(\frac{8\phi_c}{2\pi}\right) 2\pi r' dr' \left(2\pi\sin\gamma'\right) d\gamma' \\ &= 4r^2 \int_{\gamma_2}^{\gamma_3} \varpi' \cdot T\phi_c \left(2\pi\sin\gamma'\right) d\gamma'\end{aligned} \tag{3}$$

#116072 - $15.00 USD Received 24 Aug 2009; revised 6 Nov 2009; accepted 16 Nov 2009; published 23 Nov 2009

$$\Phi_{sidewall}^{circular} = \int_{\gamma_2}^{\gamma_3} \varpi' \cdot T \left[\int_0^{R_c} 2\pi r' dr' + \int_{R_c}^{r} (4\phi / 2\pi) \cdot 2\pi r' dr' \right] (2\pi \sin\gamma') d\gamma'$$
$$= 2r^2 \int_{\gamma_2}^{\gamma_3} \varpi' \cdot T \left[\arcsin\left(\frac{R_c}{r}\right) + \frac{R_c}{r}\sqrt{1-\left(\frac{R_c}{r}\right)^2} \right] (2\pi \sin\gamma') d\gamma' \quad (4)$$

whereby T is the transmission coefficient calculated from Fresnel equation:

$$T = 1 - 0.5 \times \left\{ \left[\frac{n'\cos\gamma' - n\sqrt{1-(n'\sin\gamma'/n)^2}}{n'\cos\gamma' + n\sqrt{1-(n'\sin\gamma'/n)^2}} \right]^2 + \left[\frac{n'\sqrt{1-(n'\sin\gamma'/n)^2} - n\cos\gamma'}{n'\sqrt{1-(n'\sin\gamma'/n)^2} + n\cos\gamma'} \right]^2 \right\}$$

The ratio r/R is about 0.7~0.8 in practical LED chip designs, and the emission radius r is obviously greater than the maximum R_c. In the calculations, the ratio r/R is set to 0.75, which is consistent with our ray-tracing simulations. The projected critical angle φ_c and R_c are defined in Eq. (1) and (2), and the integration limits are defined by the refractive indexes in the following equations.

$$\gamma_2 = \arcsin\frac{\sqrt{n^2-1}}{n'}$$

$$\gamma_3 = \arcsin\frac{n}{n'}$$

The definite integrals (3) and (4) are evaluated using Matlab to be 0.912 r^2 and 1.099 r^2 respectively, while the total power radiation within cone γ_2 and γ_3 are 2.291r^2. Therefore, the sidewall extraction ratio is 40% for cuboid geometry and 48% for circular geometry, giving a geometrical enhancement factor of 20.5%. This is again consistent with the ray-tracing simulation results.

While light extraction efficiency is a major benefit, another intuitive feature associated with the circular geometry is the inherent high degree of symmetry, which is attractive in applications where uniform illumination in a circular pattern is required. The near-field spatial intensity patterns generated from simulation are shown in Fig. 1(b) and 1(c), representing the side-wall modulated top surface light distribution. The circular LED emits with a pattern of axial symmetry. This feature is apparent from the experimentally measured emission profile of a circular LED. From three different observation planes the emission patterns of the circular device are almost identical, as plotted in Fig. 7(b), contrasting sharply with the varying emission patterns at different planes from a cuboid LED as shown in Fig. 7(a). The discrepancy between the measured and simulated emission patterns is attributed to additional light scattering from the sidewall which have not been taken into account in the simulations.

#116072 - $15.00 USD Received 24 Aug 2009; revised 6 Nov 2009; accepted 16 Nov 2009; published 23 Nov 2009

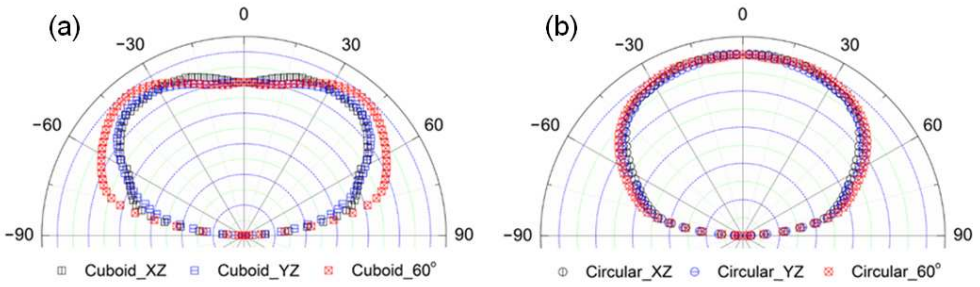

Fig. 7. Emission patterns measured from (a) cuboid and (b) circular LEDs at different vertical planes. The circular LED emits more uniformly with axial symmetry and approaches an ideal Lambertian pattern. The 60° plane corresponds to the plane derived by rotating the XZ plane by 60° angle about the Z axis.

4. Conclusion

The geometric effects of sidewall on light extraction ratio and emission pattern are studied with Monte-Carlo ray tracing simulation and mathematical modeling, together with measurement of fabricated devices shaped by laser micromachining. The circular LED demonstrated a ~20% enhancement of sidewall extraction in the simulation without considering scattering on the sidewall. Emission pattern of the fabricated circular LED is measured and exhibits a balanced Lambertian pattern. The measured 10% enhancement in overall light output from the circular LED verified the simulation results. Mechanism of enhanced sidewall extraction with a practical circular LED is discussed based on the most efficient sidewall extraction mode. From these results and our understanding, we anticipate opening up a wide range of possibilities with sidewall geometries for producing application specific LED light emitters.

#116072 - $15.00 USD Received 24 Aug 2009; revised 6 Nov 2009; accepted 16 Nov 2009; published 23 Nov 2009